

# Non-Gaussian traces in the variance from small scale CMB observations

E. Gaztañaga, P. Fosalba, E. Elizalde

Institut d'Estudis Espacials de Catalunya, Research Unit (CSIC),  
Edf. Nexus-104 - c/ Gran Capitán 2-4, 08034 Barcelona

## ABSTRACT

We compare the latest results from CMB experiments at scales around  $l_e \sim 150$  over different parts of the sky to test the hypothesis that they are drawn from a Gaussian distribution, as is usually assumed. We test different sets of strategies and find in all cases incompatibility with the Gaussian hypothesis above the one-sigma level. We next show how to include a generic non-Gaussian signal in the data analysis. Results from CMB observations can be made compatible with each other by assuming a non-Gaussian distribution for the signal, with a kurtosis at a level  $B_4 = \langle \delta_T^4 \rangle_c / \langle \delta_T^2 \rangle_c^2 \simeq 90$ . A possible interpretation for this result is that the initial fluctuations at the surface of last scattering are strongly non-Gaussian, although it could also be due either to underestimation of the systematic errors, foreground contamination, non-linear effects or a combination of them.

*Subject headings:* cosmic microwave background — cosmology:observations — methods:statistical

## 1. Introduction

A basic ingredient to understand the formation of large scale structures in our Universe is the distribution of initial conditions. Have fluctuations been generated in the standard inflationary epoch or do they require topological defects or more exotic assumptions for the initial conditions? While the former assumption typically produces a Gaussian distribution (Bardeen, Steinhardt, Turner 1983) the latter involves strong non-Gaussianities (e.g. Vilenkin 1985, Turok & Spergel 1991). This issue can be addressed both in the present day Universe fluctuations, as traced by the galaxy distribution (e.g. Silk & Juszkiewicz 1991, Gaztañaga & Mähönen 1996), or in the the anisotropies of the cosmic microwave background (CMB) (e.g. Coulson et al. 1994, Smoot et al. 1994). Here we will address the latter possibility in a somewhat indirect way.

One important contribution to the uncertainties in the measurements of the amplitude of the CMB comes from the sample variance. That is, the uncertainty due to the finite size of the observational sample. In order to estimate these sampling errors it is common practice to assume that the underlying signal is Gaussian (e.g. Bond et al. 1994). These errors are added to other sources of error to test models of structure formation or to compare between experiments. A non-Gaussian signal can produce different sampling errors, and this possibility has already been proposed as a way to reconcile the discrepancies between different experiments (Coulson et al. 1994, Luo 1995).

Here we propose to go a step further and use the estimated discrepancies or variance between different experiments to place limits on the degree of non-Gaussianity. In order to do this we will assume that the quoted systematic errors in each experiment are accurate, at least on average. We will focus on results which are either from different parts of the sky or, when over the same area, from multipoles with windows that are well separated apart. Our strategy is not to average results from a given experiment, but to find as many independent results as possible in order to have a large sampling over the underlying distribution.

## 2. Sample Variance

We want to study the sample variance of CMB experiments over independent sky regions or subsamples. We will denote the ensemble average by  $\langle \cdots \rangle$ . In each subsample we have measurements on several resolution cells or patches, whose averages (within the subsample) we denote by bars. As usual, we assume the *fair sample hypothesis* by which ensemble averages are identified with spatial averages. This implicitly assumes that the subsamples are large enough to neglect the average cross correlations between patches as compared to the mean square contributions (see, Scott et al. 1994 and references therein). In order to derive the sample variance of the temperature fluctuations in the sky for a generic non-Gaussian field, we define our radiation field as

$$\Delta_m = T_m - \bar{T}, \quad (1)$$

$T_m$  being the temperature field at a point within certain patch  $m$  over which we calculate the subsample average,  $\bar{T}$ . Notice that the actual (normalized) fluctuation field is given by

$$(\delta_T)_m = \frac{T_m - \bar{T}}{\bar{T}} = \frac{\Delta_m}{\bar{T}}. \quad (2)$$

According to this notation, all magnitudes derived from the field  $\Delta_m$  may have dimensions. To obtain adimensional variables one should conveniently scale them with the mean background temperature. It follows from its definition that the subsample average  $\bar{\Delta} = 0$ , so that its variance is:

$$\bar{\Delta}^2 = \frac{1}{N} \sum_m^N \Delta_m^2. \quad (3)$$

In the literature this quantity is denoted by  $\delta T^2$ , which should not be confused with our notation for the adimensional local fluctuation  $\delta_T$ . The sample variance of  $\bar{\Delta}^2$  is therefore the variance of the variance of the temperature field

$$\begin{aligned} Var(\delta T^2) \equiv Var(\bar{\Delta}^2) &= \langle (\bar{\Delta}^2 - \langle \bar{\Delta}^2 \rangle)^2 \rangle = \frac{1}{N^2} \langle \sum_{m,n} (\Delta_m^2 - \langle \Delta_m^2 \rangle) (\Delta_n^2 - \langle \Delta_n^2 \rangle) \rangle \\ &= \frac{1}{N^2} \left\{ \sum_m \langle (\Delta_m^2 - \langle \Delta_m^2 \rangle)^2 \rangle + \sum_{m \neq n} \langle (\Delta_m^2 - \langle \Delta_m^2 \rangle) (\Delta_n^2 - \langle \Delta_n^2 \rangle) \rangle \right\}, \quad (4) \end{aligned}$$

where we have made use of the fact that the sum commutes with the ensemble average,  $\langle \cdots \rangle$ .

Furthermore, assuming that all subsamples are large enough as for the *fair sample hypothesis* to apply, we can drop the last term and rewrite the first one, to get (using the hypothesis once more)

$$Var(\overline{\Delta^2}) = \frac{1}{N} \left\{ \langle \overline{\Delta^4} \rangle - \langle \overline{\Delta^2} \rangle^2 \right\} = \frac{1}{N} \left\{ \langle \overline{\Delta^4} \rangle_c + 2 \langle \overline{\Delta^2} \rangle_c^2 \right\}, \quad (5)$$

where we have applied the standard definition for  $\langle \dots \rangle_c$ , connected moments or cumulants (e.g. Kendall, Stuart & Ort 1987), in this case:  $\langle \overline{\Delta^2} \rangle_c^2 = \langle \overline{\Delta^2} \rangle^2$  and  $\langle \overline{\Delta^4} \rangle_c = \langle \overline{\Delta^4} \rangle - 3 \langle \overline{\Delta^2} \rangle_c^2$ .

Throughout the analysis we shall consider a general family of non-Gaussian signals with *dimensional* scaling, which is chosen because it enters at the same level than the Gaussian contribution in the sample variance and also because it is the natural output for matter fluctuations in models where the initial conditions are given by topological defects generated through a phase transition (e.g. Turok & Spergel 1991). For *dimensional* scaling, we have that the 4th order cumulant scales with the square of the 2nd order cumulant, so that:

$$B_4 \equiv \frac{\langle \overline{\Delta^4} \rangle_c}{\langle \overline{\Delta^2} \rangle_c^2} = \frac{\langle \overline{\Delta^4} \rangle_c}{\langle \overline{\Delta^2} \rangle_c^2}, \quad (6)$$

is a constant (e.g. independent of  $\langle \overline{\Delta^2} \rangle_c$ ). In terms of  $B_4$ , expression (5) then reads

$$Var(\delta T^2) \equiv Var(\overline{\Delta^2}) = \frac{1}{N} (2 + B_4) \langle \overline{\Delta^2} \rangle_c^2. \quad (7)$$

The Gaussian sample variance corresponds to the particular case  $B_4 = 0$ . It is important to stress the general applicability of (5) for non-Gaussian processes. Particular cases, such as the  $\chi_n^2$  distribution studied by Luo (1995), can be recovered by just replacing  $\langle \overline{\Delta^4} \rangle_c$  for the values in the particular distribution. For the  $\chi_n^2$  we just have  $B_4 = 12/n$  (Fosalba et al. 1997), but note that the  $\chi_n^2$  is not a good candidate as a non-Gaussian distribution, since in this case the variance is  $\langle \overline{\Delta^2} \rangle = 2/n$  which fixes  $n \simeq 10^{10}$  to match the observations  $\delta T^2 \simeq 10^{-10}$ , and gives a very small non-Gaussian signal:  $B_4 \simeq 10^{-9}$ .

### 3. Small-scale CMB Data compilation

For each CMB experiment over a given subsample, labeled  $i$ , we denote as usual

$$\delta T(i) \equiv \sqrt{(\overline{\Delta^2})_i} \quad (8)$$

ie,  $\delta T(i)$  is the *rms* temperature anisotropy, from which one estimates the band power  $\delta T_l(i)$  for every  $l$  multipole component of the power spectrum.

Table 1 shows a compilation of data from small-scale experiments for scales within the range  $90 \leq l_e \leq 200$ . This interval is specially suitable for a  $\chi^2$  analysis since it is the most densely sampled, according to observational reports. This table shows all the latest available small-scale experimental data within the range  $90 \leq l_e \leq 200$ . The scale and size of each window peaks at multipole number  $l_e$  and has a width given by the  $\pm \Delta l_e$  interval (computed as the scales at which the window falls to a factor of  $e^{-0.5}$  from the peak value). Each input in this table corresponds to independent sky patches. The total quoted error,  $\sigma_{\delta T}^G$ , includes the calibration uncertainty, the number of independent points for the statistical

used in Test	CMB experiments	$\delta T_l$ ( $\mu K$ )	$\sigma_{\delta T}^G$ ( $\mu K$ )	$\sigma_{sv}^G$ ( $\mu K$ )	$l_e$	$+\Delta l_e$	$-\Delta l_e$	$N_{points}$
A1,A2,A3,B	<sup>a</sup> MAX-GUM (3)	78	18	9	145	100	60	39
	<sup>a</sup> MAX-MUP (3)	26	10	3	145	100	60	39
	<sup>a</sup> MAX-ID (4)	46	18	7	145	100	60	21
	<sup>a</sup> MAX-SH (4)	49	19	8	145	100	60	21
	<sup>a</sup> MAX-HR5127 (5)	33	15	4	145	100	60	29
	<sup>a</sup> MAX-PH (5)	52	15	7	145	100	60	29
	<sup>b</sup> MSAM-2 beam(1)	61	37	7	159	75	76	34
	<sup>b</sup> MSAM-2 beam(2)	28	18	3	159	112	82	34
	<sup>c</sup> SK95C6	64	17	7	135	6	37	48
	<sup>c</sup> SK95C7	72	19	7	158	7	38	48
B	<sup>c</sup> SK95C5	54	17	8	108	8	32	24
	<sup>c</sup> SK95C8	81	20	8	178	6	38	48
	<sup>c</sup> SK95C9	76	20	8	197	8	37	48
	<sup>c</sup> SK94K5	44	14	6	96	21	19	24
	<sup>c</sup> SK94K6	33	15	3	115	21	19	48
	<sup>c</sup> SK94Q9	138	55	14	176	20	23	48
	<sup>d</sup> ARGO	39	6	3	98	70	38	63
	<sup>e</sup> PYTHON-III <sub>L</sub>	59	14	3	178	61	45	158
	<sup>e</sup> PYTHON-III <sub>S</sub>	54	14	3	92	7	39	127

Table 1: Available small-scale experimental data within the range  $90 \leq l_e \leq 200$ .

analysis given by the independent bins in RA in each observation. The data essentially follows Ratra & Sugiyama 1995, but several cases are taken from the original observational reports. Notice that performing the correct window weighting of the CMB models (e.g. in Ratra et al. 1997) hardly changes the final results within the errors and, therefore, the flat band hypothesis that we are using for comparing individual experiments should be equally accurate.

The superscript *a* in Table 1 denotes the MAX experiments (see Tanaka et al. 1995, and references therein). They are labeled according to the sky patch and flight, MAX-*Sky patch (flight)*; *b* denotes the two MSAM1-94 (single difference) experiments reported in Cheng et al. 1996, referring to independent sky regions in RA; *c* denotes the *Saskatoon'95* experiments, where SK95Cn correspond to the CAP region around the NCP, SK94Kn and SK94Qn corresponds to the K and Q band experiments for the *Saskatoon'94* flight, with the *n* point chopping strategy in each case (see Netterfield et al 1997); *d*, is the ARGO experiment (see De Bernardis et al. 1994); *e* denotes PYTHON-III<sub>L</sub> and PYTHON-III<sub>S</sub> for the subtractive large and small chop-window measurements, respectively (see, Platt et al. 1996). The data points with their errors (horizontal ones corresponding to the window width) are displayed in Figure 1 .

In the above results, Gaussian (G) statistis have been assumed to calculate the sampling variance contribution to the error and this is always included in the quoted errors. For a general non-Gaussian case

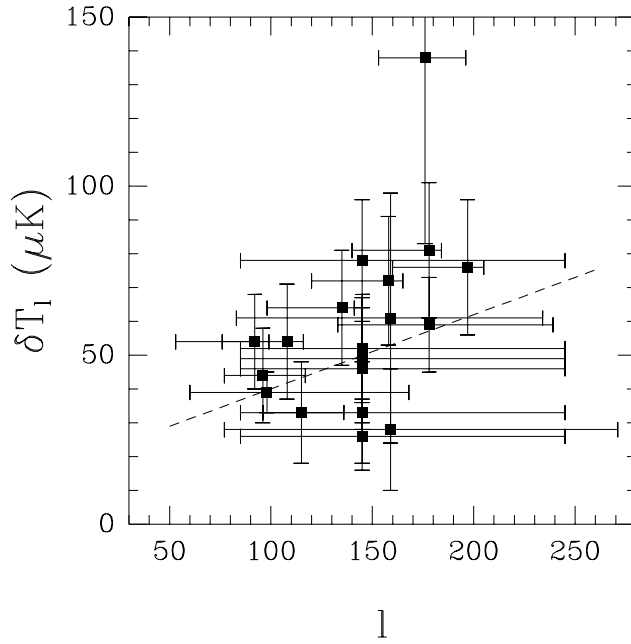


Fig. 1.— Band power estimates of the *rms* temperature anisotropy  $\delta T_l$  for observations given in Table 1. The vertical error bars show the (symmetrized) total errors in  $\delta T_l$  while the horizontal ones stand for the width of the windows. The dashed line is the best fit slope to the data,  $\delta T_l = (11/50)l_e + 18$ .

we would like to replace this contribution with the more general expression given above. We will assume that the remaining contribution to the error is truly Gaussian. The sampling variance estimation in the experiments is usually done with Gaussian Monte-Carlo simulations. Here, to estimate this contribution we will use its theoretical expectation. We first write the rms error  $\sigma_{sv}$  from the sampling variance as:

$$\sigma_{sv}[\delta T^2] = \left[ \text{Var}(\delta T^2) \right]^{1/2} = 2 \delta T \sigma_{sv}[\delta T], \quad (9)$$

so that, for a Gaussian ( $B_4 = 0$ ), we find from equation (7) that:

$$\sigma_{sv}[\delta T] = \sqrt{\frac{1}{2N} \left( 1 + \frac{B_4}{2} \right)} \delta T, \quad (10)$$

were  $N$  is the number of independent observations. In this equation, we have used the individual experiment (or subsample) averages  $\delta T$  instead of the *ensemble* averages:  $\langle \Delta^2 \rangle_c$ . This is not exact, but reproduces better what is done in each experiment to estimate the Gaussian sampling error, which we denote  $\sigma_{sv}^G$  (i.e., for  $B_4 = 0$  above). We have checked that the results shown below do not significantly depend on such approximation. We then assume that the total error for a Gaussian signal  $\sigma_{\delta T}^G$ , given in the observational reports, can be obtained by adding in quadrature  $\sigma_{sv}^G$  to the other errors (e.g. the instrumental and calibration errors). The values of  $\sigma_{\delta T}^G$  and  $\sigma_{sv}^G$  for each experiment are shown in Table 1.

We next carry out a Chi-square analysis taking different number of points according to the following criteria:

- **Test A:** Taking a band as narrow and densely sampled as possible, so that we can neglect any dependence of the signal with the scale,  $l$ . We consider three cases with increasing number of points: **A1, A2, A3**: which correspond to the first 6, 8&10 points of Table 1, respectively, starting with the MAX experiments alone.
- **Test B:** Taking a wider band, as densely sampled as possible, and computing the  $\chi^2$  value with **(B1)** and without **(B2)** a linear fit to the signal with  $l_e$ , i.e. removing a possible scale dependence of the power spectrum in the analysis.

Table 2 displays the  $\chi^2$  values for all the cases involved in approaches **A** and **B**. DOF denotes the number of degrees of freedom:  $N - 3$  (two parameters are correlated to the data: the mean and  $B_4$ ) for all cases, except for the last case where  $\text{DOF} = N - 4$  —since the slope incorporates one extra parameter to the computation.

The  $\chi^2$  values are obtained from:

$$\chi^2 = \sum_i \left( \frac{\langle \delta T_l \rangle - \delta T_l(i)}{\sigma_{\delta T}(i)} \right)^2, \quad (11)$$

were  $\delta T_l(i)$  and  $\sigma_{\delta T}(i)$  are the individual values in Table 1. The mean  $\langle \delta T_l \rangle$  in each test is estimated from the individual values  $\delta T_l(i)$  weighted by the inverse of the variance  $\sigma_{\delta T}^2(i)$ , which produces the minimum  $\chi^2$  possible. The values of the  $\chi^2$  and  $\langle \delta T_l \rangle$  shown in Table 2 correspond to the Gaussian case,  $B_4 = 0$ , and  $\sigma_{\delta T} = \sigma_{\delta T}^G$ . In the last test we find that the best fit linear relation,  $\langle \delta T_l \rangle = a l_e + b$ , that minimizes the  $\chi^2$  is found for  $a \simeq 11/50$  and  $b \simeq 18$ . All cases considered show a disagreement with the Gaussian hypothesis above the  $1\sigma$  level of significance.

For a non-Gaussian signal, the total error above,  $\sigma_{\delta T}$ , should include the sampling variance for the corresponding non-Gaussian distribution, in equation (10), as well as the instrumental and calibration

Test	Experiments	$\chi^2/\text{DOF}$	Significance	$\langle \delta T_l \rangle (\mu K)$	
		Gaussian case ( $B_4 = 0$ )		Non-Gaussian $B_4$	
<b>A1</b>	MAX	7.6/3	about $2\sigma$	41.5	58 – 548
<b>A2</b>	MAX+MSAM	8.4/5	well above $1\sigma$	40.7	16 – 238
<b>A3</b>	MAX+MSAM+SK95C6 & 7	12.2/7	well above $1\sigma$	45.1	34 – 276
<b>B1</b>	ALL	23.9/16	about $2\sigma$	46.3	22 – 140
<b>B2</b>	ALL with slope	20.0/15	above $1\sigma$	$(11/50)l_e + 18$	31 – 171

Table 2:  $\chi^2$  analysis of combined experiments.

errors. This can be simply related to the total (Gaussian) error  $\sigma_{\delta T}^G$ , quoted in Table 1, by :

$$\sigma_{\delta T}(i) = \sigma_{\delta T}^G(i) \left[ 1 + \frac{B_4}{8N_i^2 (\sigma_{\delta T}^G(i)/\delta T_l(i))^4} \right]^{1/2}. \quad (12)$$

The range for the non-Gaussian parameters  $B_4$  shown in Table 2 are the values needed to produce a  $\chi^2$  value corresponding to an interval of confidence between 25%-75%. This range narrows as the number of data points increases, but the mean values are always away from zero.

Note that our approach is not totally consistent. We are assuming a non-Gaussian distribution for the signal but we determine the confidence intervals using the  $\chi^2$  distribution, which assumes a Gaussian likelihood. The whole analysis improves substantially by repeating it in terms of a non-Gaussian likelihood function. In the limit  $\chi^2 \gg N$  and small variance, it is possible to relate the Gaussian confidence intervals with the corresponding non-Gaussian ones in terms of  $B_4$  and  $B_3^2$ , where  $B_3 = \langle \delta_T^3 \rangle_c / \langle \delta_T^2 \rangle_c^{3/2}$  (see Amendola 1996). This can be done by using the Edgeworth series to expand an arbitrary non-Gaussian distribution around a Gaussian in terms of its cumulants (e.g. Juszkiewicz et al. 1995). Within the limitation that  $\chi^2 \gg N \gg 1$  (which restricts applicability to Test **B** only), it turns out that the confidence intervals obtained above are widened —when the non-Gaussian corrections are taken into account— by a factor between 1.2 and 2 [i.e.  $1/(1+q)$ , given by Eq. (15) in Amendola 1996]. To do this estimation one has to assume something for the value of  $B_3^2$ . The later factors correspond to  $B_3 = 0$  and  $B_4$  in Table 2, which is the most conservative case. This increases the significance to well above  $2\sigma$  for both of the Test **B** cases in Table 2. Fosalba et al. (1997) have found that typical values of  $B_3$  in several non-Gaussian distributions with *dimensional* scaling lie just below  $B_3^2 = B_4$ . For each assumed value of  $B_3$  we can now find in a consistent way the values of  $B_4$  needed in the  $\chi^2$  to get an interval of confidence between 25%-75% in the non-Gaussian likelihood. For  $|B_3| = 8 \lesssim B_4^{1/2}$ , the allowed ranges for  $B_4$  corresponding to Test **B1** and **B2** on Table 2 shrink to  $B_4 = 70 - 90$  and  $B_4 = 90 - 130$ . The improvement in this case is quite remarkable, but the range of allowed values of  $B_4$  increases as  $B_3$  approaches zero.

#### 4. Discussion

Our analysis shows that using the quoted error bars in different CBM experiments, for scales within the range  $90 \leq l_e \leq 200$ , they can only be made compatible with each other by assuming a non-Gaussian distribution for the signal, with a kurtosis at a level of  $B_4 = \langle \delta_T^4 \rangle_c / \langle \delta_T^2 \rangle_c^2 \simeq 90$ . As the mean signal is defined to obtain the minimum  $\chi^2$ , any comparison with models could only lead to a more significant disagreement. The Gaussian weighted mean  $\langle \delta T_l \rangle$ , shown in Table 2, becomes lower with the non-Gaussian hypothesis, although this is only significant for Test **A**, with small number of points, where the reduction can be up to 15%.

A possible interpretation for this result is that the initial fluctuations at the surface of last scattering are strongly non-Gaussian. Even if this initial distribution were purely Gaussian, it is not clear yet how non-linear effects in the CMB fluctuations or reionization (e.g. Dodelson & Jubas 1995) would change the final observed distributions, although the calculations for some of the relevant effects indicate only mildly deviations with cumulants of *hierarchical* type (see e.g. Mollerach et al. 1995, Munshi et al.

1995). Other possibilities include foreground contamination, which could be in the form of large spots that should typically induce non-Gaussian fluctuations (although de Oliveira-Costa et al. 1997, found this contamination to reduce the Saskatoon normalization by only 2%).

Besides the *dimensional* scaling  $\langle \delta_T^4 \rangle_c = B_4 \langle \delta_T^2 \rangle_c^2$ , we have also consider another family of non-Gaussian models: the case of the *hierarchical* scaling, where  $\langle \delta_T^4 \rangle_c = S_4 \langle \delta_T^2 \rangle_c^3$  which is the natural outcome of gravitational growth for matter fluctuations (e.g. Peebles 1980). Thus, the two models are related by  $B_4 = S_4 \langle \delta_T^2 \rangle_c$ . We have done a similar analysis for the *hierarchical* case and found that the corresponding values of the non-Gaussian parameters are  $S_4 \simeq 10^{12}$ . As the variance  $\delta T^2$  is roughly constant in this analysis, this value agrees well with the naïve expectation:  $S_4 \simeq B_4 / \delta T^2 \simeq B_4 \times 10^{10}$ .

Within the large parameter space for non-Gaussian distributions, the values we find for  $B_4$  and  $S_4$  lie in the strongly non-Gaussian cases. In typical non-Gaussian models with *hierarchical* scaling one has  $S_4 \lesssim 10^2$  (e.g. Fosalba et al. 1997), much smaller than our result  $S_4 \simeq 10^{12}$ . For matter fluctuations,  $\delta_m$ , gravitational growth from Gaussian initial conditions also gives  $S_4$  of order 10 – 100 (e.g. Bernardeau 1994, Gaztañaga & Baugh 1995).

For non-Gaussian initial conditions, the topological defects from phase transitions, like textures (e.g. Turok & Spergel 1991), predict  $B_4 \simeq 1$ , for  $\delta_m$ , and have been measured around this value in N-body simulations (Gaztañaga & Mähönen 1996), while in the present study we get values around  $B_4 \simeq 90$ . Thus, the estimated amplitudes for  $B_4$  and  $S_4$  seem to indicate high levels of non-Gaussianity, at least according to  $\delta_m$  standards. Note that, in principle, one would expect lower levels of non-Gaussianity in  $\delta_T$  than in  $\delta_m$ , as the former comes as an integrated effect, at least on large scales (see Scherrer & Schaefer 1995).

The large difference in the order of magnitudes between  $S_4 \simeq 10^{12}$  and  $B_4 \simeq 10^2$  indicates that *dimensional* scaling is a more adequate representation for our findings than the *hierarchical* one. If this is the case one would also typically expect a non-vanishing value for  $B_3$  of order  $B_3^2 \lesssim B_4$  (Fosalba et al. 1997). In this case we can put a very tight constraint on  $B_4$  to lie between  $B_4 = 70 - 90$ , for a flat power spectrum, or  $B_4 = 90 - 130$  for the best fitted slope in Table 2.

E.G. and P.F. wish to thank Scott Dodelson for encouraging discussions and the Fermilab group for their kind hospitality during our visit in the fall 1996, where this project started. E.G. acknowledges support from CIRIT (Generalitat de Catalunya) grant 1996BEAI300192. This work has been supported by CSIC, DGICYT (Spain), project PB93-0035, and CIRIT, grant GR94-8001.

## REFERENCES

Amendola, L., 1996, Astro. Lett. and Comm. 33, 63  
 Bernardeau, F., 1994 A & A, 291, 697  
 Bardeen, J.M., Steinhardt, P.J., Turner, M.S., 1983 Phys.Rev. D,28 679  
 Bond, J.R., Crittenden, R., Davis, R.L., Efstathiou, G., Steinhardt, P.J., 1994, Phys.Rev.Lett.,72, 13  
 Cheng, E.S., et al. 1994, Ap. J. (Letters), 422, L37

Cheng, E.S., et al. 1996, 456, L71

Clapp, A.C., et al. 1994, Ap. J. (Letters), 433, L57

Coulson, D., Ferreira, P., Graham P., Turok, N., 1994, Nature, 368, 27

De Bernardis et al. 1994, Ap. J. (Letters), 422, L33

de Oliveira-Costa, et al. , 1997, astro-ph/9705090

Devlin, M.J., et al. 1994, Ap. J. (Letters), 430, L1

Dodelson, S., Jubas, J.M., 1995 ApJ, 439, 503

Fosalba, P., Gaztañaga, E., Elizalde, E., 1997, in preparation

Gaztañaga, E., Baugh, C.M., 1995, MNRAS, 273, L1

Gaztañaga, E., Mähönen, P., 1996, Ap. J. (Letters), 462, L1

Gundersen, J.O., et al. 1993, Ap. J. (Letters), 413, L1

Juszkiewicz, R., Weinberg, D.H., Amsterdamski, P., Chodorowski, M., Bouchet, F.R., 1995, ApJ, 442, 39

Kendall, M., Stuart, A. Ort, J.K., 1987, Kendall's Advanced Theory of Statistics, Oxford University Press

Luo, X., 1995, ApJ, 439, 517

Netterfield, C.B., Devlin, M.J., Jarosik, N., Page, L., Wollack, E.J., 1997, ApJ, 474, 47

Mollerach, S., Gangui, A., Lucchin, F., Matarrese, S., 1995, ApJ, 453, 1

Munshi, D., Souradeep, T., Starobinsky, A., 1995, ApJ, 454, 556

Platt, S.R., Kovac, J., Dragovan, M., Peterson, J.B., Ruhl, J.E., 1996, astro-ph/9606175

Ratra, B., Sugiyama, N., 1995, astro-ph/9512157

Ratra, B., Banday, A.J., Górsky, K.M., Sugiyama, N., 1995 astro-ph/9512148

Rocha, G., Hancock, S., 1996, astro-ph/9611228

Ruhl, J.E., et al. 1995, Ap. J. (Letters), 453, L1

Scherrer, R.J., Schaefer R.K., 1995, ApJ, 446, 44

Scott, D., Srednicki, M., White, M., 1994 Ap. J. (Letters), 421, L5

Silk J., Juszkiewicz, R. 1991, Nature, 353, 386

Smoot, G.F., Banday, A.J., Kogut, A., Wright, E.L., Hinshaw, G., Bennett, C.L. 1994, ApJ, 437, 1

Tanaka, S.T. et al. 1995, astro-ph/9512067

Turok N., Spergel, D.N., 1991 Phys.Rev.Lett.,66, 3093

Peebles, P.J.E., 1980, *The Large Scale Structure of the Universe*: Princeton University Press

Vilenkin, A., Phys.Rep.121, 263